Anomalous and planar Hall effect of orthorhombic and tetragonal $SrRuO_3$ layers

M. Ziese*
Division of Superconductivity and Magnetism, University of Leipzig, D-04103 Leipzig, Germany

I. Vrejoiu†
Max Planck Institute of Microstructure Physics, D-06120 Halle, Germany

(Received 18 March 2011; revised manuscript received 11 July 2011; published 8 September 2011)

High quality $Pr_{0.7}Ca_{0.3}MnO_3/SrRuO_3$ superlattices were fabricated by pulsed laser deposition. The $SrRuO_3$ layers grew either in orthorhombic or tetragonal symmetry depending on the thickness of the $Pr_{0.7}Ca_{0.3}MnO_3$ layers. Since the $Pr_{0.7}Ca_{0.3}MnO_3$ layers were insulating at low temperatures, magnetotransport measurements of the superlattices allowed for the measurement of the anomalous and planar Hall effect of the $SrRuO_3$ layers. The easy axis direction was found to be close to the surface normal, $[110]_o$ direction, in the case of orthorhombic $SrRuO_3$, but in plane along $\langle 110\rangle_t$ in the case of tetragonal $SrRuO_3$. The anomalous Hall effect in both the orthorhombic and tetragonal phases can be understood within the intrinsic Berry-phase mechanism. The carrier density was 1.5 and 1.25 electrons per formula unit in the orthorhombic and tetragonal phase, respectively.

DOI: 10.1103/PhysRevB.84.104413 PACS number(s): 75.70.Ak, 75.60.−d, 75.47.Lx

I. INTRODUCTION

Epitaxial heterostructures and superlattices (SLs) of perovskite oxides offer a multitude of pathways to modify the crystalline and magnetic structure of the constituent layers. Recently it was shown that the crystalline symmetry of $SrRuO_3$ layers in $Pr_{0.7}Ca_{0.3}MnO_3/SrRuO_3$ superlattices depended on the thickness of the $Pr_{0.7}Ca_{0.3}MnO_3$ (PCMO) layers, although the $SrRuO_3$ (SRO) layer thickness was constant.[1] On increase of the PCMO layer thickness from 1.5 to 4.0 nm the crystalline symmetry of 4-nm-thick SRO layers changed from orthorhombic to tetragonal.[1] It was further shown that a weak antiferromagnetic interlayer coupling is present between the ferromagnetic SRO layers (Curie temperature $T_C \simeq 145$ K) and the weakly ferromagnetic PCMO layers ($T_C \simeq 115$ K).[2] This is similar to the case of $La_{0.7}Sr_{0.3}MnO_3/SrRuO_3$ SLs and bilayers that show strong antiferromagnetic interlayer coupling.[3–7] Since PCMO is insulating, the conductivity of the PCMO/SRO SLs is determined by the conducting SRO layers. This opens up the possibility to probe the magnetotransport properties of orthorhombic and tetragonal SRO layers by measuring on the SLs.

The anomalous Hall effect of $SrRuO_3$ has attracted considerable interest in recent years, since its unusual temperature dependence has been attributed to the intrinsic Berry phase mechanism[8] combined with a magnetic-monopole-like structure in momentum space.[9–11] This interpretation, however, has been contested and the behavior of the anomalous Hall effect was also found compatible with an extrinsic mechanism for the anomalous Hall effect;[12] moreover, the emergence of a superstructure modulation below 60 K might affect the Hall conductivity.[13] In any case, $SrRuO_3$ is of general interest for the understanding of anomalous Hall-effect mechanisms, since it does not show a scaling between off-diagonal and diagonal conductivity tensor components, $\sigma_{xy} \propto \sigma_{xx}^{\alpha}$, as found for other oxide and non-oxide ferromagnets,[14] especially $La_{0.7}Sr_{0.3}MnO_3$,[15,16] CrO_2,[17] and Fe_3O_4,[18] as well as being predicted theoretically.[8] Hall-effect measurements on tetragonal SRO samples are crucial for a further understanding, since the Berry-phase mechanism was predicted to distinctly depend on the crystal symmetry.[9]

In this work we review the structural and magnetic properties of the PCMO/SRO SLs. We then focus on the resistivity and the Hall effect of the SRO layers in the SLs compared to SRO single films. The change in the SRO crystal structure from orthorhombic to tetragonal modifies the directions of the magnetic easy and hard axes, while maintaining the large magnetocrystalline anisotropy. Further, this structure modification eliminates the sign change in the anomalous Hall constant characteristic for orthorhombic SRO. The implications for the Hall-effect mechanism in SRO are discussed.

II. EXPERIMENT

PCMO/SRO SLs, single PCMO, and SRO films were fabricated by pulsed laser deposition (248 nm, KrF laser) from polycrystalline targets. The substrate temperature was 650 °C and the oxygen partial pressure was 0.14 mbar. Vicinal $SrTiO_3(001)$ substrates with a miscut angle of about 0.1°, uniform TiO_2 termination, and an atomically flat terrace morphology were used. The microstructure of the SLs was investigated by transmission electron microscopy (TEM), atomic force microscopy, and x-ray diffractometry. The SLs grew in the step-flow growth regime and were very smooth with a mean-square roughness of 0.4 nm, i.e., one unit cell.

The magnetic properties of the SLs were investigated by superconducting quantum interference device magnetometry with the magnetic field applied both parallel and perpendicular to the SL normal. The magnetic moments were normalized to the total volume of the SLs and were expressed in Bohr magneton per unit cell using an average unit-cell size of $(0.39\ \text{nm})^3$. Resistivity and anomalous and planar Hall effect were measured in van der Pauw geometry in magnetic fields up to 8 T and temperatures up to 300 K. Two SLs and two single SRO films were chosen for the Hall-effect measurements; see Table I. Single PCMO films were weakly ferromagnetic with

TABLE I. Layer thicknesses and Curie temperatures of the SLs. Curie temperatures of the PCMO layers were determined from magnetization, those of the SRO layers from resistivity measurements. Sample SL1 had orthorhombic, SL3 tetragonal SRO layers.

Sample	$(PCMO/SRO)_{15}$	T_C (K) (SRO)	T_C (K) (PCMO)
SL1	(1.5 nm/4.4 nm)	143	≃110
SL3	(3.8 nm/4.0 nm)	142	≃115
SR1	(0/5.0 nm)	143	
SR2	(0/40 nm)	145	

a Curie temperature in the range 110–115 K.[2] For an extensive characterization of the SRO films, see [19].

III. RESULTS

A. Structural characterization

Figure 1 shows θ-2θ scans close to the substrate STO (002) reflection for both SLs. The PCMO (002) reflection is visible for SL3 with the 3.8-nm-thick PCMO layers, but not for SL1 with the 1.5-nm-thin PCMO layers, either due to the insufficient resolution of the x-ray diffractometer or due to fully strained growth of the very thin PCMO layers. The SRO (002) reflection is buried by the substrate reflection for both SLs. Both samples show clear satellite reflections at least up to the second order. From the satellite reflexes the SL periods were determined as 6.9 ± 0.2 and 7.9 ± 0.2 nm for SLs SL1 and SL3, respectively. The PCMO layers of SL3 have an out-of-plane lattice constant of 0.385 nm.

An extensive TEM characterization was presented elsewhere.[1] From this as well as from magnetoresistance measurements it was found that the PCMO layers were orthorhombic in both SLs, whereas the SRO layers had orthorhombic symmetry in SL1 and tetragonal symmetry in SL3.[1] With respect to the cubic $SrTiO_3(001)_c$ substrate the orthorhombic SRO layers had an epitaxial relation with $[110]_o \parallel [001]_c$, $[001]_o \parallel [100]_c$, $[1\bar{1}0]_o \parallel [010]_c$, and the

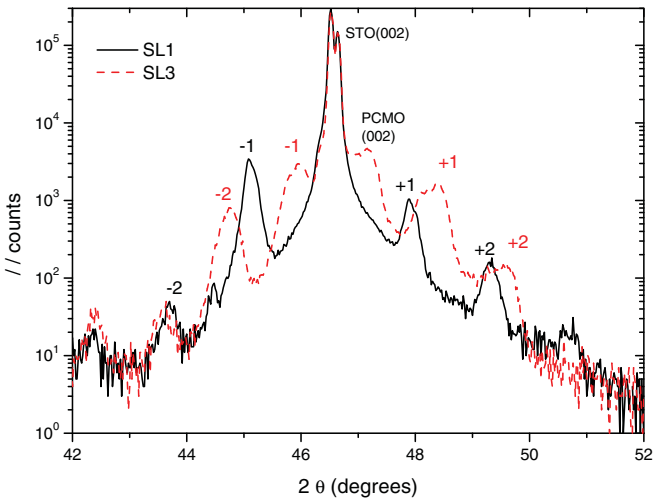

FIG. 1. (Color online) θ-2θ scan near the STO (002) reflection clearly showing satellite reflections from the superlattice.

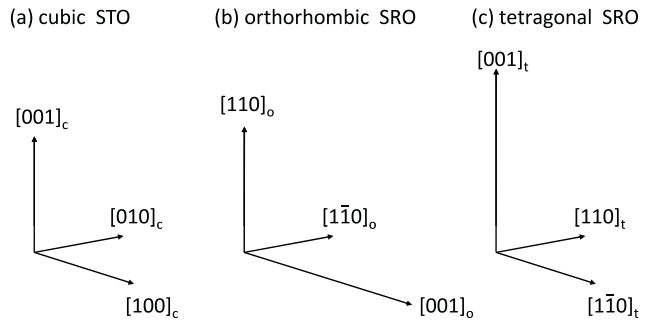

FIG. 2. Relative orientation of the (a) cubic STO, (b) the orthorhombic SRO, and (c) the tetragonal SRO unit cell.

tetragonal SRO layers with $[001]_t \parallel [001]_c$, $[1\bar{1}0]_t \parallel [100]_c$, $[110]_t \parallel [010]_c$. This is schematically illustrated in Fig. 2. The PCMO layers grew with $[110]_o \parallel [001]_c$, but showed two crystallographic domains with $[001]_o$ either along $[100]_c$ or $[010]_c$.

B. Magnetization

Magnetization vs temperature curves measured under various magnetic fields applied parallel and perpendicular to the SLs are shown in Fig. 3. The magnetization was measured on field cooling from 200 K. Both SLs showed a strong

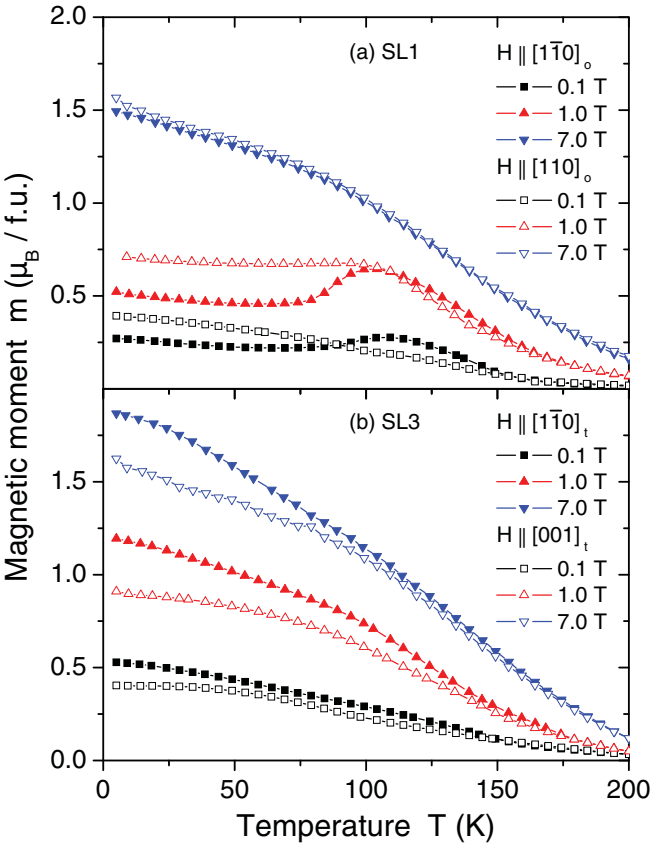

FIG. 3. (Color online) High-field magnetization vs temperature curves of SLs (a) SL1 and (b) SL3 for both in-plane (solid symbols) and out-of-plane (open symbols) magnetic fields (f.u. = formula unit).

magnetic-field dependence of the magnetization with no sign of saturation even in 7 T. In the case of SL3 the magnetization measured in magnetic fields applied parallel to the SL was always larger than that measured in perpendicular fields. This showed that the substrate normal was the magnetic hard axis in this SL.

SL1 showed a more complex behavior. In applied fields of 0.1 and 1.0 T a maximum was observed in the in-plane magnetization. This is a signature of antiferromagnetic (AF) interlayer coupling between the SRO and the PCMO layers occurring below the Curie temperature of the PCMO layers of 110 K.[2] Since the out-of-plane magnetization is larger than the in-plane magnetization at low temperatures, the magnetic easy axis might be along or near the SL normal. For comparison, the easy axis of orthorhombic SRO single films makes an angle of about 30° with the $[110]_o$ direction.[19,20] Overall, the magnetization data indicate that there is AF interlayer exchange coupling in the SLs; this is, however, so weak in SL3 that it was not observable in magnetic fields of 0.1 T and higher. The strength of the AF interlayer coupling appears to be larger in SL1 with orthorhombic SRO layers than in SL3 with tetragonal SRO layers.[2] This might be understood by a favorable spin alignment. Since the *b* axis is the easy direction of ferromagnetic PCMO,[21] and since the *b* axis makes an angle of 45° with the surface normal, the spin directions of Mn and Ru interfacial spins make a smaller relative angle for orthorhombic than for tetragonal SRO, since the latter has in-plane magnetic easy axes (see below).

C. Resistivity

The in-plane resistivity of SLs SL1 and SL3 as well as the SRO single films SR1 and SR2 are shown in Fig. 4 in comparison to the in-plane resistivity of a 5-nm-thick single PCMO film grown on $SrTiO_3$. The resistivity of the PCMO film is orders of magnitude larger than that of the SLs; the latter is comparable, but somewhat larger than the resistivity of SRO single films.[19,22,23] Accordingly, the resistivity of the SLs was certainly dominated by the resistivity of the conducting SRO layers, although interfacial conductivity at the PCMO/SRO interface could not be ruled out. The resistivity of the SLs showed a clear change in slope at the Curie temperature of the SRO layers; this change in slope was used to determine the Curie temperature values in Table I. The resistivity is lowest for the 40-nm-thick SRO single film and increases for the thinner film and the SLs. This might be due to a larger contribution from surface scattering in the superlattices and in sample SR1. Moreover, the microstructure of samples SR1 and SR2 is different:[19] whereas SR2 shows misfit dislocations on a scale of a few μm, SR1 is coherently strained; SR2 has a coherent orientation of the in-plane $[001]_o$ axis, whereas SR1 does not. The comparatively large resistivity of SL3 might further be related to the different crystallographic symmetry as a similar resistivity enhancement is also seen in tetragonal SRO single films.[24]

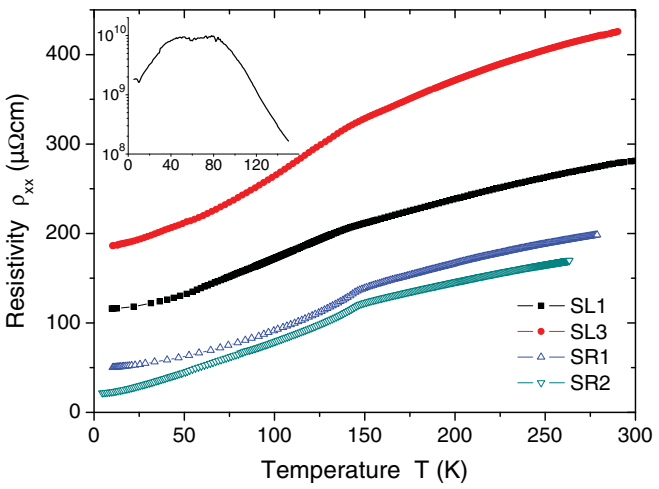

FIG. 4. (Color online) Resistivity of superlattices SL1 and SL3 and the SRO films SR1 and SR2. The inset shows the resistivity of a 5-nm-thick PCMO film for comparison; axis units are identical to those of the main image.

D. Magnetocrystalline anisotropy

1. From the anomalous Hall effect

Since the resistivity of the SLs was dominated by the resistivity of the SRO layers, the Hall resistivity was also expected to reflect the Hall resistivity of the SRO layers. The Hall resistivity ρ_{yx} was measured at various temperatures as a function of magnetic field applied perpendicular to the SL. The current direction was diagonal across square samples with the $[100]_c$ and $[010]_c$ directions of the STO substrate along the sample edges. Therefore the current density was along the $[100]_t$ direction in the case of sample SL3 with tetragonal SRO layers and at an angle of 45° with respect to the $[001]_o$ direction in the case of sample SL1 with orthorhombic SRO layers.

The anomalous Hall effect follows the phenomenological law[25]

$$\rho_{yx} = \mu_0 (R_H H + R_A M_\perp), \tag{1}$$

where R_H denotes the ordinary, R_A the anomalous Hall coefficient, H the applied field, and $M_\perp$ the magnetization component perpendicular to the SL. Note that for thin films and SLs the demagnetizing factor along the SL normal is close to unity such that the magnetic induction is equal to the applied magnetic field, $B = \mu_0 H$. In the case of the superlattices the Hall resistivity was used to monitor the SRO layer magnetization only.

Hall resistivity data measured at 10, 110, and 150 K are shown in Fig. 5. At low temperatures SL1 showed a ferromagnetic loop due to the anomalous Hall effect superimposed onto a straight line, following Eq. (1). The small dips seen at 10 K and ±1.6 T are attributed to the antiferromagnetic interlayer coupling leading to an intricate magnetic reversal mechanism. The Hall resistivity of SL3 is shown in Fig. 5(b). The magnetic-field dependence of the Hall resistivity of this SL was completely different than that of SL1; this was directly due to the change in crystalline symmetry. The *S*-like contribution to the anomalous Hall effect is typical for ferromagnetic films having a hard axis along the film normal.[26] This shows that the SL normal was the magnetic hard axis of SL3, whereas the Hall-effect loop shape of SL1 indicates that the magnetic easy axis is close to the SL normal in agreement with literature.[19,20]

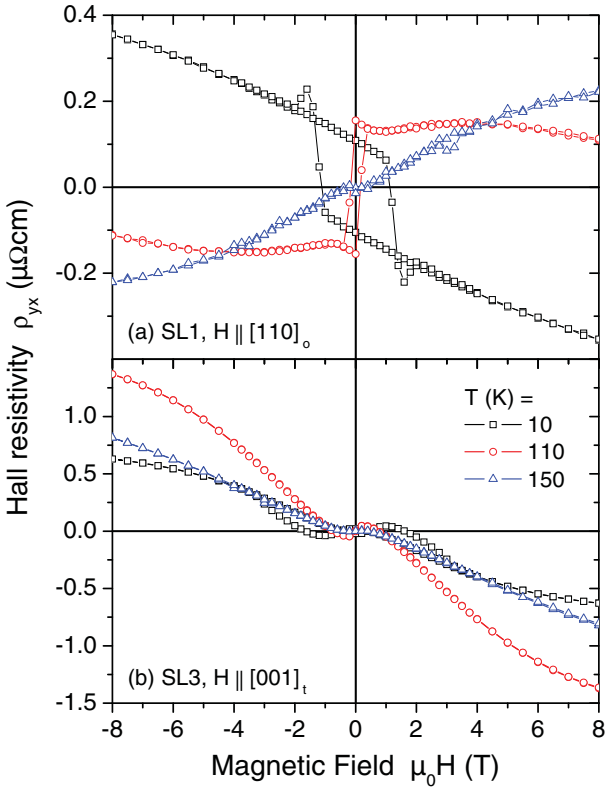

FIG. 5. (Color online) Hall resistivity ρ_{yx} of SLs (a) SL1 and (b) SL3 as a function of applied field for temperatures 10, 110, and 150 K.

The angle dependence of the Hall resistivity for rotation of the magnetic field in the $(001)_o$ plane of SL1 and the $(110)_t$ plane of SL3 is shown in Fig. 6. Since the magnetocrystalline anisotropy of SRO is rather large of the order of 500 kJ/m^3,[19] the magnetization vector is in general not aligned with the magnetic-field vector in an applied field of 8 T. Therefore hysteresis appeared in the angle dependent Hall resistivity curves close to a magnetic hard axis, since there the magnetization vector did not follow the field vector any more. In the case of SL1 hysteresis was observed around -33° indicating the location of a magnetic hard axis in the $(001)_o$ plane, 33° away from the $[1\bar{1}0]_o$ direction toward the $[110]_o$ direction. This is consistent with magnetoresistance measurements on single SRO films.[19] In the case of SL3 hysteresis was observed around $[001]_t$, i.e., around the SL normal. In this case the magnetic hard axis is along the SL normal as also indicated by the magnetization and field dependent Hall-effect measurements above.

2. *From the planar Hall effect*

The planar Hall effect was measured for rotation of a magnetic field $\mu_0 H = 8$ T within the SL basal plane and is shown in Fig. 7 for temperatures of 10, 50, and 110 K. In the case of SL1 a pronounced hysteresis appeared around the $[001]_o$ direction that is known to be a magnetic hard axis.[19,27] In this sample spurious hysteresis was also observed around the $[1\bar{1}0]_o$ direction, although this is not a magnetic hard axis; however, it is close to the magnetic hard axis found in the $(001)_o$ plane 33° away from the $[1\bar{1}0]_o$ direction. In the case of

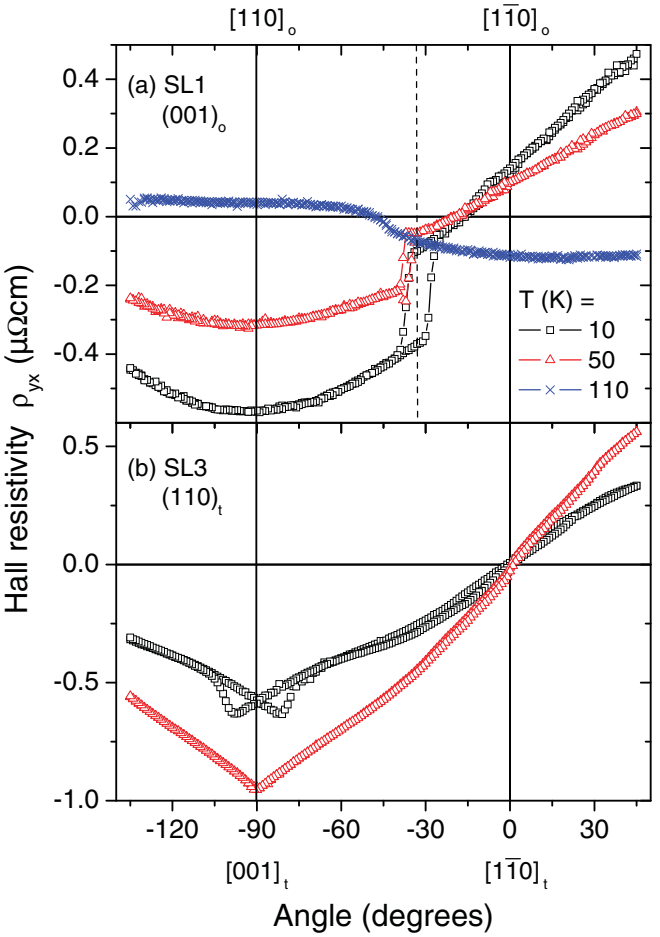

FIG. 6. (Color online) Angle dependence of the Hall resistivity of (a) SL1 for field rotation in the $(001)_o$ plane and (b) SL3 for field rotation in the $(110)_t$ plane. Applied field was $\mu_0 H = 8$ T.

SL3 hysteresis was found around -45°, i.e., a magnetic hard axis is located along the $[100]_t$ direction.

The planar Hall effect had a magnitude of up to 0.02 $\mu\Omega$ cm and was apparently larger in the orthorhombic than in the tetragonal phase. In the case of SL1 with orthorhombic SRO layers the planar Hall effect is likely to contain a sizable contribution from the anomalous Hall effect, since the magnetization is likely to have some component along the easy axis perpendicular to the layers. The planar Hall effect observed here is significantly smaller than in Ref. 28 and is far from having the "giant" values reported for $La_{0.84}Sr_{0.16}MnO_3$ (Ref. 29) and Fe_3O_4 (Refs. 30–32) films.

E. Origin of the anomalous Hall effect

Following Eq. (1) the high-field slope of the Hall effect was determined in the field range between 6 and 8 T. The subtraction of the high-field slope left a Hall contribution with a curve shape similar to a magnetization loop. $\mu_0 R_A M_A$ was then determined by extrapolation of the flat part of the corrected Hall resistivity to $H = 0$.[10,25] For samples SL1, SR1, and SR3 these values are shown as a function of temperature in Fig. 8(a). Common features are discernible for these samples, namely a negative value of the anomalous Hall constant at low temperatures, followed by a sign change and a maximum

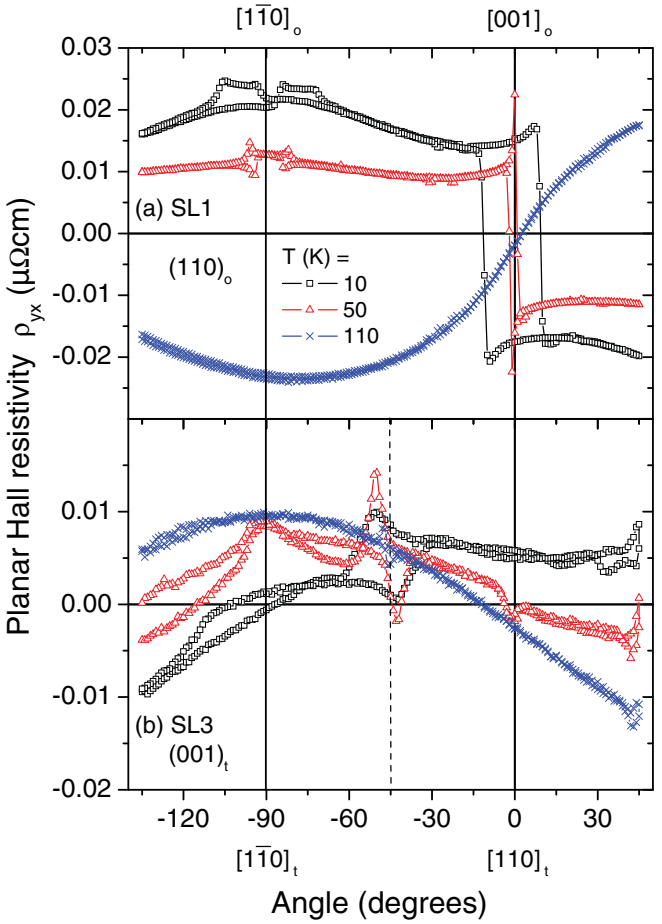

FIG. 7. (Color online) Planar Hall effect of SLs (a) SL1 and (b) SL3. The applied field $\mu_0 H = 8$ T was rotated in the (a) $(110)_o$ and (b) $(001)_t$ planes, respectively.

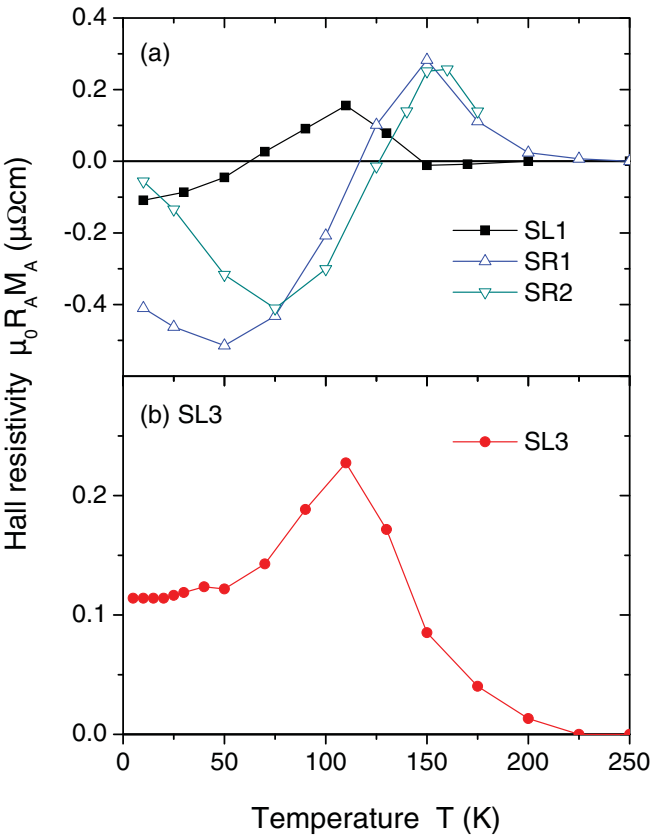

FIG. 8. (Color online) Extrapolated anomalous Hall resistivity ($\mu_0 R_A M_S$) as a function of temperature for (a) SL1 and SRO single films SR1 and SR2 and (b) SL3.

at higher temperatures, albeit the exact temperatures of these features vary from sample to sample. In contrast, $\mu_0 R_A M_A$ of sample SL3 with tetragonal SRO layers is positive throughout the measured temperature regime. One should keep in mind that M_A is a magnetization obtained by an extrapolation procedure and that $M_A \to 0$ above the Curie temperature. The data obtained here are in qualitative agreement with the data of Refs. 10–13,33, and 34. The vanishing of the sign change in the anomalous Hall constant with a change in crystalline symmetry might indicate its relation to the band structure;[9,10] see discussion below.

Under the assumption that the magnetization saturates at high fields, the high-field slope of the Hall resistivity is equal to the ordinary Hall contribution $\mu_0 R_H H$. Figure 9(a) shows this apparent R_H for the four samples as a function of temperature. In the case of the orthorhombic SRO layers R_H shows a sign change, whereas for sample SL3 R_H is negative throughout the temperature range studied. The sign change has been reported before.[13,27] In a two-band model the sign change would correspond to a change from electron in the ferromagnetic to hole conduction in the paramagnetic phase.[35] This appears, however, unlikely, since the resistivity does not show any anomalies and since the assumption that the magnetization is saturated in an applied field of 8 T is not valid close to and above the Curie temperature. Moreover, for sample SL3 the out-of-plane direction is magnetically hard and it might be doubtful whether the magnetization is saturated in this sample at any temperature. Within measurement error R_H saturates for $T \to 0$. Within a one-band model the saturation value yields a carrier density of about 1.5 electrons/f.u. for samples SL1, SR1, and SR2 and of about 1.25 electrons/f.u. for sample SL3. These values are sensible[35,36] and the former value is in agreement with Refs. 13 and 37. Therefore we regard the extrapolated values as good estimates of the carrier density in the samples. Since SRO is a metal, the carrier density is likely to be temperature independent in the investigated temperature range[10,12] such that the temperature dependence of the high-field slope might be attributed to the anomalous Hall effect. Below the Curie temperature the anomalous Hall constant R_A can be determined from the measured values of the remanent magnetization and of $R_A M_A$, above the Curie temperature R_A can be determined from the high-field slope $\mu_0(R_H + R_A \chi)H$ and the measured paramagnetic susceptibility χ. This yields the anomalous Hall constant R_A shown in Fig. 9(b). For this R_H was approximated by its low-temperature value, the susceptibility was determined from the measured magnetization [$\chi = \chi_0 T_C/(T - T_C)$ with $\chi_0 = 0.0028, 0.0025$, $T_C = 140, 155$ K for samples SR1 and SR2, respectively; the magnetization for SL1 and SL3 was approximated by that of sample SR1]. The resulting anomalous Hall constant R_A shows a sign change for orthorhombic SRO and is positive throughout for tetragonal SRO. At higher

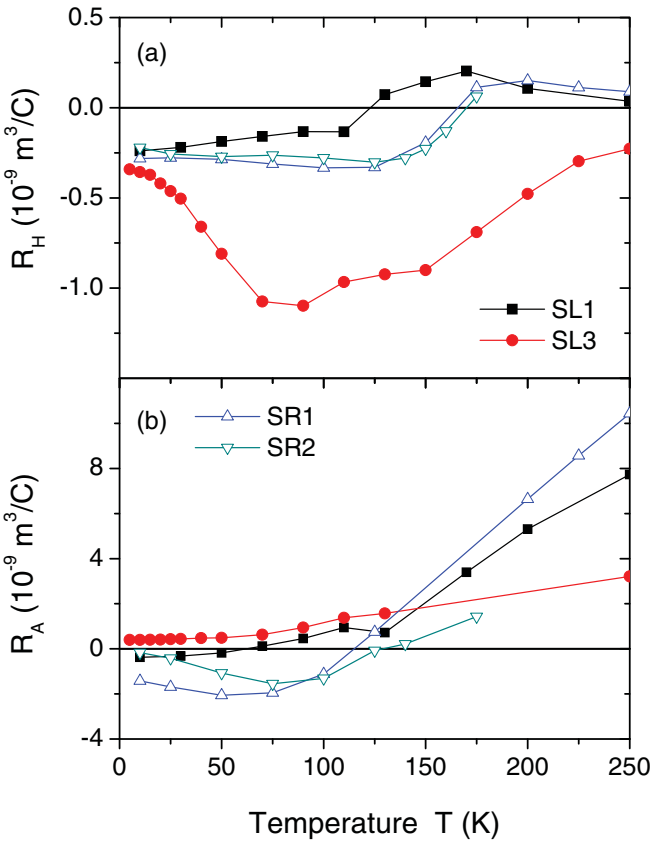

FIG. 9. (Color online) (a) Apparent ordinary Hall constant R_H and (b) anomalous Hall constant R_A as a function of temperature.

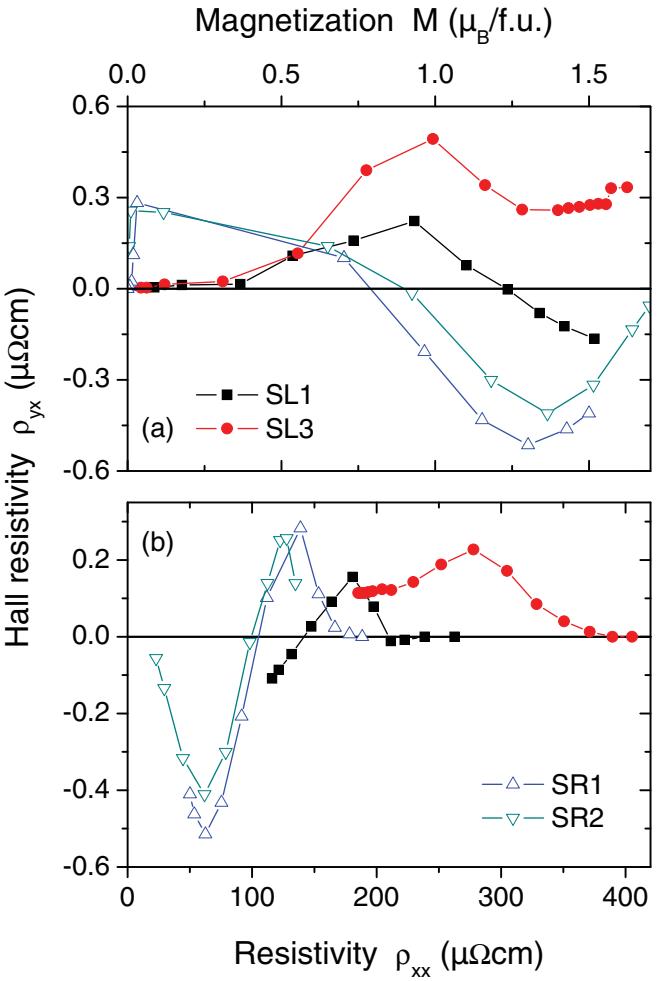

FIG. 10. (Color online) (a) Hall resistivity ρ_{yx} as a function of (a) magnetization and (b) longitudinal resistivity ρ_{xx}.

temperatures R_A increases approximately linearly; the data are in qualitative agreement with those in Ref. 12.

The anomalous Hall effect of $SrRuO_3$ has received much attention in recent years, since its nonsimple temperature dependence[12,33] was related either to the intrinsic anomalous Hall contribution and magnetic monopoles in momentum space[9–11,34] or to low-temperature structural phase transitions.[13] Based on the theory of the intrinsic Hall effect supplemented by band-structure calculations for $SrRuO_3$ a scaling relation between the Hall conductivity $\sigma_{xy} \simeq \rho_{yx}/\rho_{xx}^2$ and the magnetization was proposed.[9] In the case of our samples the measured Hall resistivity ρ_{yx} was of the same magnitude, whereas the longitudinal resistivity ρ_{xx} varied rather strongly from sample to sample; see Fig. 4. Therefore we did not find a scaling of Hall conductivity with magnetization; instead the Hall resistivity is shown as a function of magnetization in Fig. 10(a). In the case of superlattices SL1 and SL3 the Hall resistivity ρ_{yx} measured at 7 T and corrected for the normal contribution is shown vs the magnetization measured in 7 T, in the case of films SR1 and SR2 the extrapolated Hall resistivity values are plotted vs the remanent magnetization. The single SRO films SR1 and SR2 tend to follow a universal curve, whereas the superlattices show different behavior: SL1 still shows a sign change, SL3 branches away above a magnetization value of about $0.5\mu_B$/f.u. The latter behavior follows the trend indicated in Ref. 9 that the low-temperature sign of the anomalous Hall effect is different for orthorhombic and cubic symmetry, and can be viewed as a corroboration of the Berry-phase mechanism.

The extrinsic mechanisms for the anomalous Hall effect predict another kind of scaling relation, i.e., $\rho_{yx} \propto \rho_{xx}$ for skew scattering[38] and $\rho_{yx} \propto \rho_{xx}^2$ for side-jump scattering.[39] Indeed this dependence is found in certain samples.[26,40] Figure 10(b) shows the corresponding scaling plot ρ_{yx} vs ρ_{xx}. Although samples SR1 and SR2 again scale quite well, no scaling is observed for the superlattices. Moreover, none of the curves follows the scaling relationship for the extrinsic contribution $a\rho_{xx} + b\rho_{xx}^2$ with temperature-dependent coefficients a and b.

From the comparison of these scaling approaches the intrinsic mechanism appears to describe the data more appropriately. Especially this mechanism might be able to explain the absence of the sign change in R_A for tetragonal $SrRuO_3$ by band-structure modifications when changing the crystalline symmetry. However, in orthorhombic $SrRuO_3$ high-resolution x-ray-diffraction provided evidence for a superstructure modulation below 200 K that might be related to the magnetic ordering and that splits below about 60 K.[13] This structural modulation has to be taken into account before the intrinsic Hall-effect picture might provide full agreement with the data.

IV. CONCLUSIONS

High quality PCMO/SRO superlattices were grown on $SrTiO_3$ substrates by pulsed laser deposition. Depending on the thickness of the PCMO layers the SRO layers had either orthorhombic or tetragonal crystalline symmetry. Strong antiferromagnetic interlayer exchange coupling between SRO and PCMO layers was observed in the superlattice with orthorhombic SRO layers. The Hall resistivity and planar Hall effect of superlattices with orthorhombic and tetragonal layers were measured. From the angle dependence of the Hall effect the magnetically hard axis directions were determined as $[001]_o$ for the orthorhombic and as $\langle 100\rangle_t$ for the tetragonal SRO layers. The ordinary and anomalous Hall constants depended on the crystalline symmetry. For both crystalline symmetries electron conduction with carrier densities of about 1.5 electrons/f.u. (orthorhombic) and 1.25 electrons/f.u. (tetragonal) were found. The sign change in the anomalous Hall constant observed for the orthorhombic structure was absent in the tetragonal structure. This is in agreement with a scaling analysis and provides further evidence for the predominance of the intrinsic Berry-phase Hall-effect mechanism in $SrRuO_3$.

The structural transition of the SRO layers might be driven by strain, but might also be influenced by changes in the electronic structure. Since the antiferromagnetic interlayer coupling is weakened by the orthorhombic-to-tetragonal transition,[2] magnetic coupling effects are unlikely to play a role in triggering the structural transition. The changes in the electronic structure reported here, however, might have some impact on the structural transition. This has to be elucidated in further experimental and theoretical work.

ACKNOWLEDGMENTS

This work was supported by the German Science Foundation (DFG) within the Collaborative Research Center SFB 762 "Functionality of Oxide Interfaces". We thank A. Setzer for performing the x-ray measurements and D. Hesse as well as J. Henk for a critical reading of the manuscript.

*ziese@physik.uni-leipzig.de
†vrejoiu@mpi-halle.de

[1] M. Ziese, I. Vrejoiu, E. Pippel, A. Haehnel, E. Nikulina, and D. Hesse, J. Phys. D: Appl. Phys. **44**, 345001 (2011).
[2] M. Ziese, I. Vrejoiu, E. Pippel, E. Nikulina, and D. Hesse, Appl. Phys. Lett. **98**, 132504 (2011).
[3] M. Ziese, I. Vrejoiu, E. Pippel, P. Esquinazi, D. Hesse, C. Etz, J. Henk, A. Ernst, I. V. Maznichenko, W. Hergert, and I. Mertig, Phys. Rev. Lett. **104**, 167203 (2010).
[4] X. Ke, M. S. Rzchowski, L. J. Belenky, and C. B. Eom, Appl. Phys. Lett. **84**, 5458 (2004).
[5] X. Ke, L. J. Belenky, C. B. Eom, and M. S. Rzchowski, J. Appl. Phys. **97**, 10K115 (2005).
[6] P. Padhan, W. Prellier, and R. C. Budhani, Appl. Phys. Lett. **88**, 192509 (2006).
[7] Y. Lee, B. Caes, and B. Harmon, J. Alloys Compd. **450**, 1 (2008).
[8] N. Nagaosa, J. Sinova, S. Onoda, A. H. MacDonald, and N. P. Ong, Rev. Mod. Phys. **82**, 1539 (2010).
[9] Z. Fang, N. Nagaosa, K. S. Takahashi, A. Asamitsu, R. Mathieu, T. Ogasawara, H. Yamada, M. Kawasaki, Y. Tokura, and K. Terakura, Science **302**, 92 (2003).
[10] R. Mathieu, A. Asamitsu, H. Yamada, K. S. Takahashi, M. Kawasaki, Z. Fang, N. Nagaosa, and Y. Tokura, Phys. Rev. Lett. **93**, 016602 (2004).
[11] R. Shimano, Y. Ikebe, K. S. Takahashi, M. Kawasaki, N. Nagaosa, and Y. Tokura, Europhys. Lett. **95**, 17002 (2011).
[12] Y. Kats, I. Genish, L. Klein, J. W. Reiner, and M. R. Beasley, Phys. Rev. B **70**, 180407(R) (2004).
[13] Y. Kobayashi, M. Iwata, T. Kaneko, K. Sato, K. Asai, and H. Ohsumi, Phys. Rev. B **82**, 174430 (2010).
[14] T. Miyasato, N. Abe, T. Fujii, A. Asamitsu, S. Onoda, Y. Onose, N. Nagaosa, and Y. Tokura, Phys. Rev. Lett. **99**, 086602 (2007).
[15] S. H. Chun, M. B. Salamon, Y. Lyanda-Geller, P. M. Goldbart, and P. D. Han, Phys. Rev. Lett. **84**, 757 (2000).
[16] Y. Lyanda-Geller, S. H. Chun, M. B. Salamon, P. M. Goldbart, P. D. Han, Y. Tomioka, A. Asamitsu, and Y. Tokura, Phys. Rev. B **63**, 184426 (2001).
[17] W. R. Branford, K. A. Yates, E. Barkhoudarov, J. D. Moore, K. Morrison, F. Magnus, Y. Miyoshi, P. M. Sousa, O. Conde, A. J. Silvestre, and L. F. Cohen, Phys. Rev. Lett. **102**, 227201 (2009).
[18] A. Fernández-Pacheco, J. M. De Teresa, J. Orna, L. Morellon, P. A. Algarabel, J. A. Pardo, and M. R. Ibarra, Phys. Rev. B **77**, 100403(R) (2008).
[19] M. Ziese, I. Vrejoiu, and D. Hesse, Phys. Rev. B **81**, 184418 (2010).
[20] S. Kolesnik, Y. Z. Yoo, O. Chmaissem, B. Dabrowski, T. Maxwell, C. W. Kimball, and A. P. Genis, J. Appl. Phys. **99**, 08F501 (2006).
[21] Z. Jirák, S. Krupička, Z. Šimša, M. Dlouhá, and S. Vratislav, J. Magn. Magn. Mater. **53**, 153 (1985).
[22] L. Klein, J. S. Dodge, C. H. Ahn, G. J. Snyder, T. H. Geballe, M. R. Beasley, and A. Kapitulnik, Phys. Rev. Lett. **77**, 2774 (1996).
[23] L. Klein, J. S. Dodge, C. H. Ahn, J. W. Reiner, L. Mieville, T. H. Geballe, M. R. Beasley, and A. Kapitulnik, J. Phys.: Condens. Matter **8**, 10111 (1996).
[24] A. Vailionis, W. Siemons, and G. Koster, Appl. Phys. Lett. **93**, 051909 (2008).
[25] E. M. Pugh and N. Rostoker, Rev. Mod. Phys. **25**, 151 (1953).
[26] M. Ziese and C. Srinitiwarawong, Europhys. Lett. **45**, 256 (1999).
[27] G. Cao, S. McCall, M. Shepard, J. E. Crow, and R. P. Guertin, Phys. Rev. B **56**, 321 (1997).
[28] Y. Shperber, I. Genish, J. W. Reiner, and L. Klein, J. Appl. Phys. **105**, 07B106 (2009).
[29] Y. Bason, L. Klein, J.-B. Yau, X. Hong, and C. H. Ahn, Appl. Phys. Lett. **84**, 2593 (2004).
[30] A. Fernández-Pacheco, J. M. De Teresa, J. Orna, L. Morellon, P. A. Algarabel, J. A. Pardo, M. R. Ibarra, C. Magen, and E. Snoeck, Phys. Rev. B **78**, 212402 (2008).
[31] X. Jin, R. Ramos, Y. Zhou, C. McEvoy, and I. V. Shvets, J. Appl. Phys. **99**, 08C509 (2006).

[32] Y. Bason, L. Klein, H. Q. Wang, J. Hoffman, X. Hong, V. E. Henrich, and C. H. Ahn, J. Appl. Phys. **101**, 09J507 (2007).
[33] L. Klein, J. R. Reiner, T. H. Geballe, M. R. Beasley, and A. Kapitulnik, Phys. Rev. B **61**, R7842 (2000).
[34] R. Mathieu, C. U. Jung, H. Yamada, A. Asamitsu, M. Kawasaki, and Y. Tokura, Phys. Rev. B **72**, 064436 (2005).
[35] I. I. Mazin and D. J. Singh, Phys. Rev. B **56**, 2556 (1997).
[36] P. B. Allen, H. Berger, O. Chauvet, L. Forro, T. Jarlborg, A. Junod, B. Revaz, and G. Santi, Phys. Rev. B **53**, 4393 (1996).
[37] Y. Kats, *Extraordinary Hall Effect in* $SrRuO_3$, Ph.D. thesis Bar Ilan University, Ramat Gan, 2004.
[38] J. Smit, Physica **21**, 877 (1955).
[39] L. Berger, Phys. Rev. B **2**, 4559 (1970).
[40] C. Zeng, Y. Yao, Q. Niu, and H. H. Weitering, Phys. Rev. Lett. **96**, 037204 (2006).